

Particle Flow and Heat Transfer in Fluidized Bed-in-Tube Solar Receivers

LABORATOIRE
PROCÉDÉS, MATÉRIAUX
et ENERGIE SOLAIRE
UPR 8521 du CNRS,
conventionnée avec
l'université de Perpignan
PROCESSES, MATERIALS
and SOLAR ENERGY
LABORATORY



SolarPACES conference
October 3, 2019 - Daegu

*A. Le Gal, B. Grange, R.
Gueguen, M. Donovan, J-Y
Peroy, G. Flamant*

PROMES-CNRS



- Presentation of the Next-CSP project
- Objectives of the study
- Particle flow in tube
 - Heat transfer
 - Conclusion
 - Future developments

10 partners, one objective :

*Improving the reliability and performance of concentrated solar power plants through the development and integration of a new technology based on the use of fluidized particles in tube as heat transfer fluid and storage medium.
(TRL 5)*



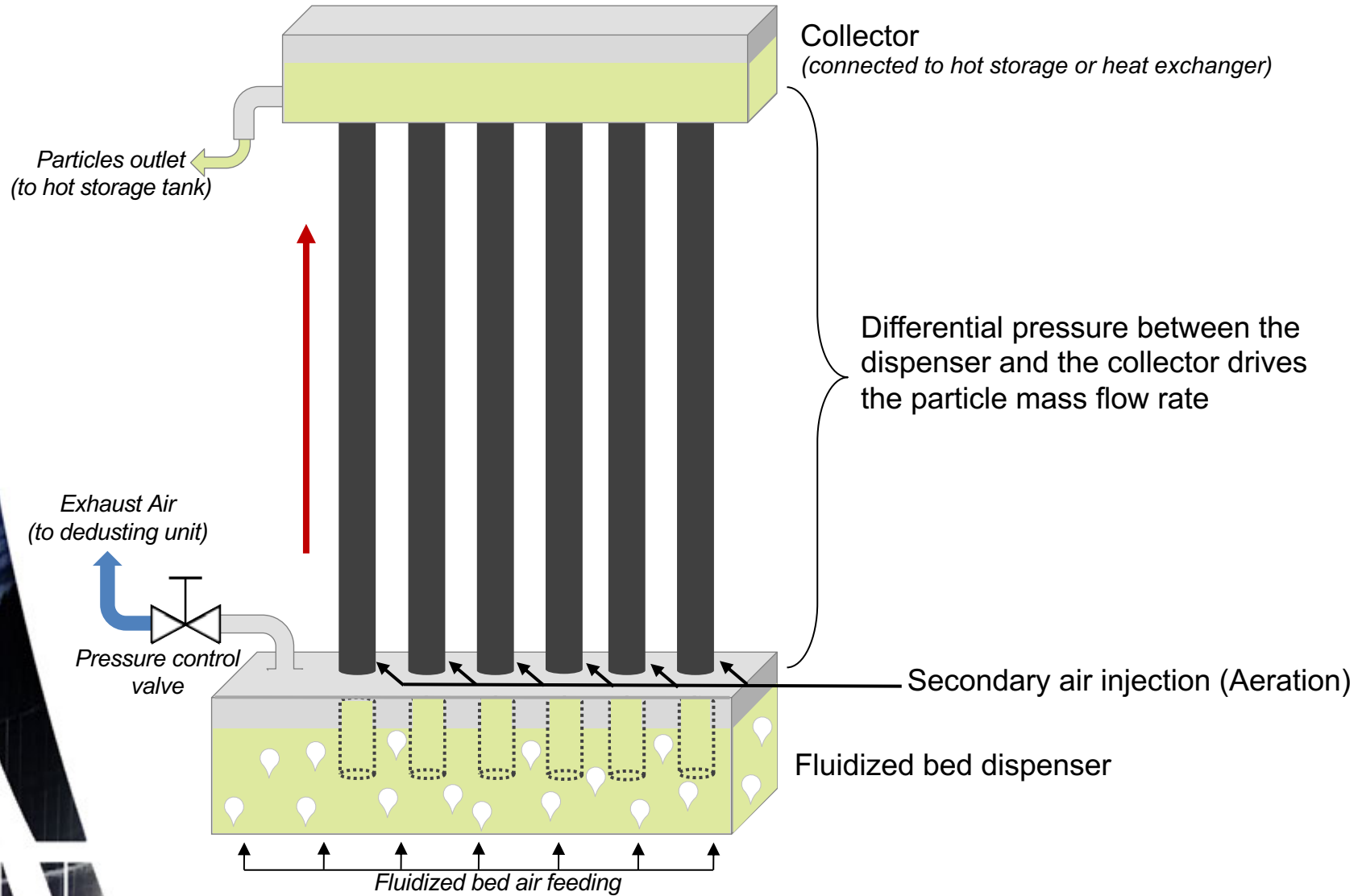
Themis solar facility - Targassonne



1MW Solar furnace - Odeillo



Upward flowing dense particle suspension solar receiver :

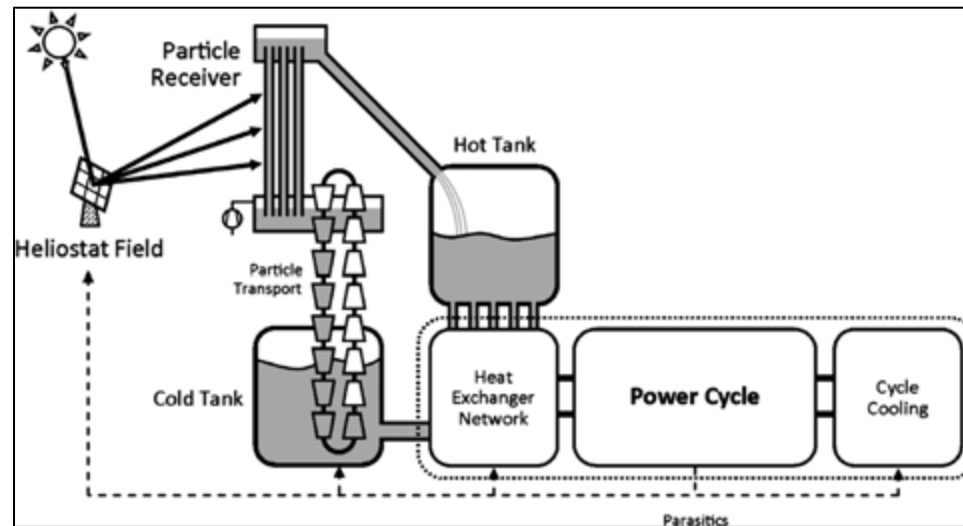


Advantages of this concept :

- Possibility to reach higher temperature than conventional heat transfer fluids (*temperature up to 750°C could considerably improve the thermodynamic cycle efficiency*)
- Direct storage of heat through the heat transfer fluid
- No freezing problems
- Good scalability of the concept (multi-tubular solar receiver)

Drawback:

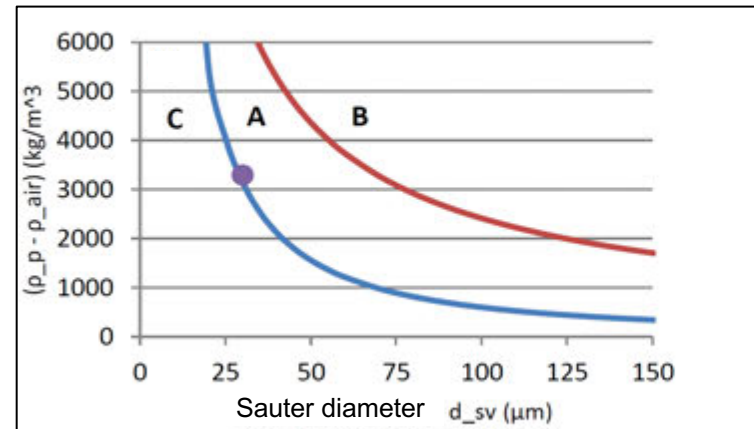
- Limited heat exchange between particles and the receiver wall surface



Generic layout of the dense particle suspension power plant. [1]

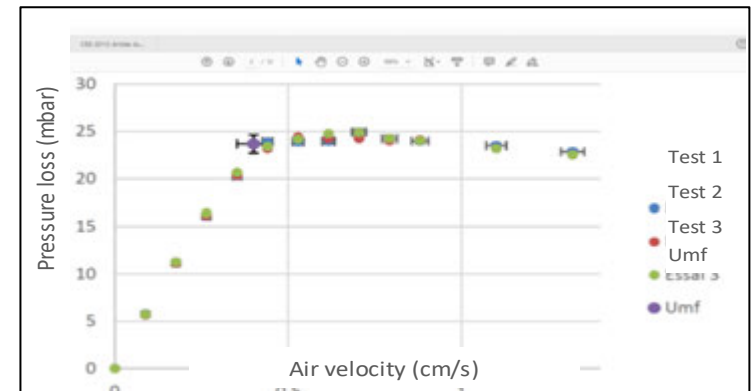
Olivine particles :

Particle	Composition	Mean diameter (d_{50}) - μm	Sauter diameter (d_{32}) - μm	Density - kg/m^3	Bulk conductivity at 800°C – W/mK
Olivine	MgO 49.5%, SiO ₂ 42%, Fe ₂ O ₃ 7.5%	59	30	3300	0.56



Geldart classification of the selected olivine particles

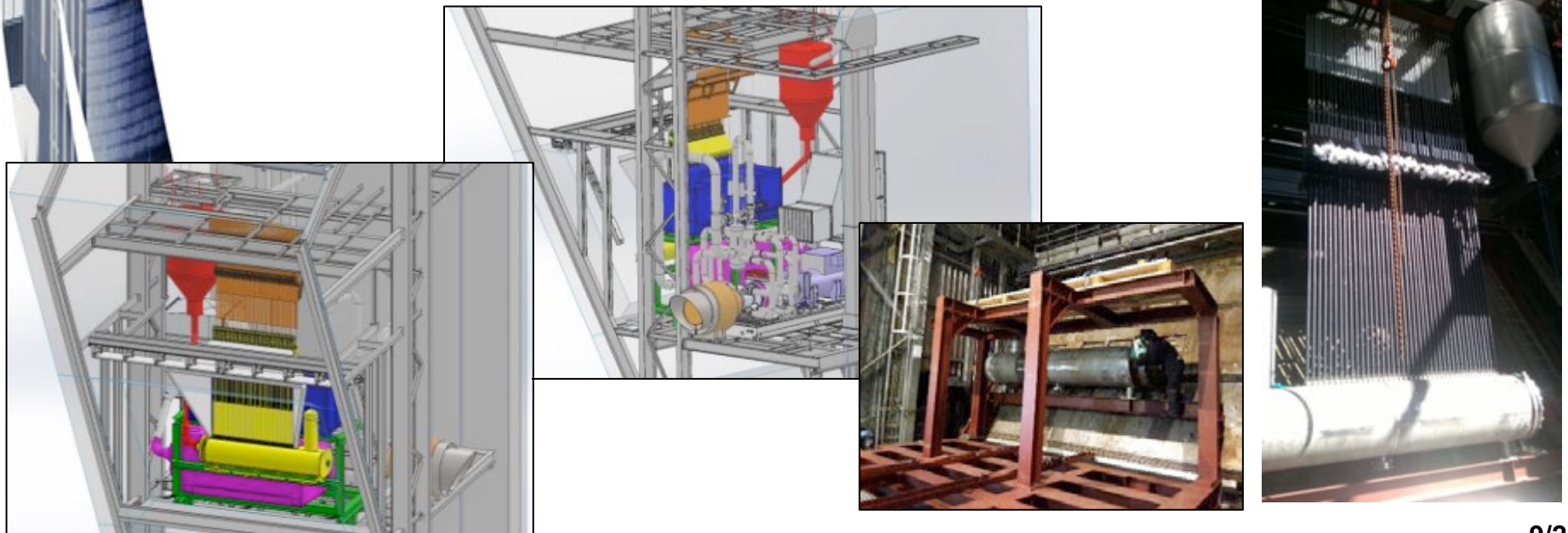
- Selected Olivine particles are part of the group A in the Geldart classification.
- The minimum air velocity to fluidized the particles is $U_{mf} = 0.40 \text{ cm/s}$



Determination of the olivine particles minimum fluidization velocity (U_{mf}).

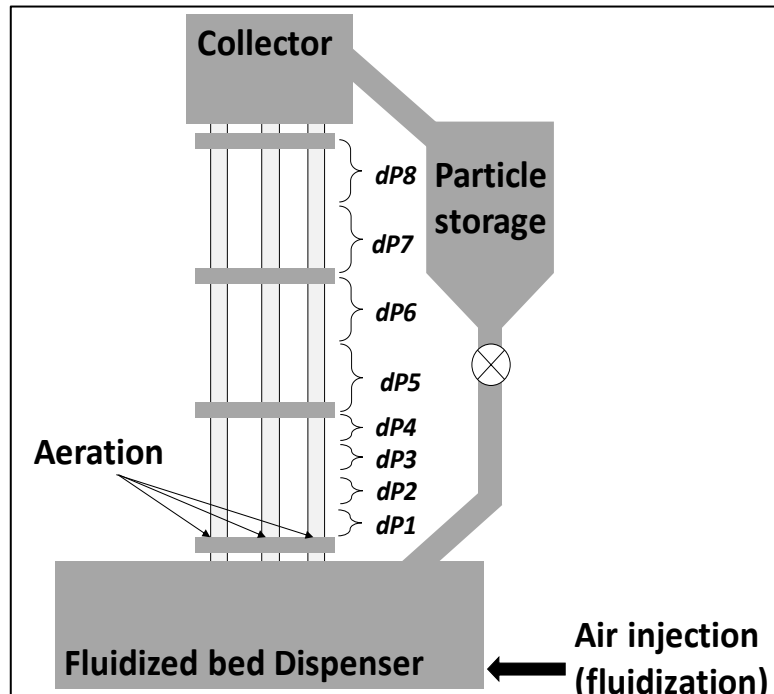
- A 3MW pilot plant is under assembly at the top of the THEMIS solar tower to demonstrate this technology in a relevant environment. (cf. Poster B-12, *B. Grange et al.*)
- The scaling up of this concept needs researches on the gas-particle flow structure evolution along tubes and on wall-to-fluidized particles heat transfer.
- In addition to modeling and simulation, two experimental mock-up were implemented to define the best operational conditions for the full scale test unit.

Needs to have a better understanding of particle flow in tube and heat transfer



« Cold » experimental setup :

- Three vertical transparent tubes (3-meters long) plunged into a fluidized bed dispenser and connected to storage tanks at the outlet.
- Uniform gas injection in the dispenser through a porous distribution plate.
- A second air injection (Aeration) placed at the tubes bottom to increase the airflow rate inside the tubes and stabilize the particle flow
- Pressure control valve in the dispenser to drive the particle flowrate
- Equipped with differential pressure gauges along the tubes
- A weighting scale implemented to measure the particle flowrate.



Particle volume fraction calculation :

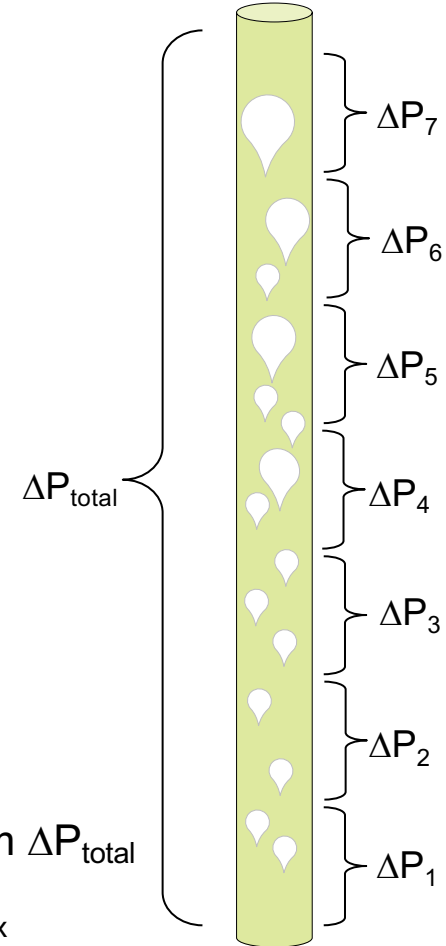
Particle volume fraction are calculated from pressure drop measurements using the following formula :

$$\Delta P = (\alpha_p \cdot \rho_p + \varepsilon \cdot \rho_g) \cdot g \cdot (h_{top} - h_{bottom})$$

$$\rightarrow \alpha_p = 1 - \varepsilon = \frac{\Delta P}{\rho_p \cdot g \cdot (h_{top} - h_{bottom})}$$

Pressure losses due to friction at the wall are neglected

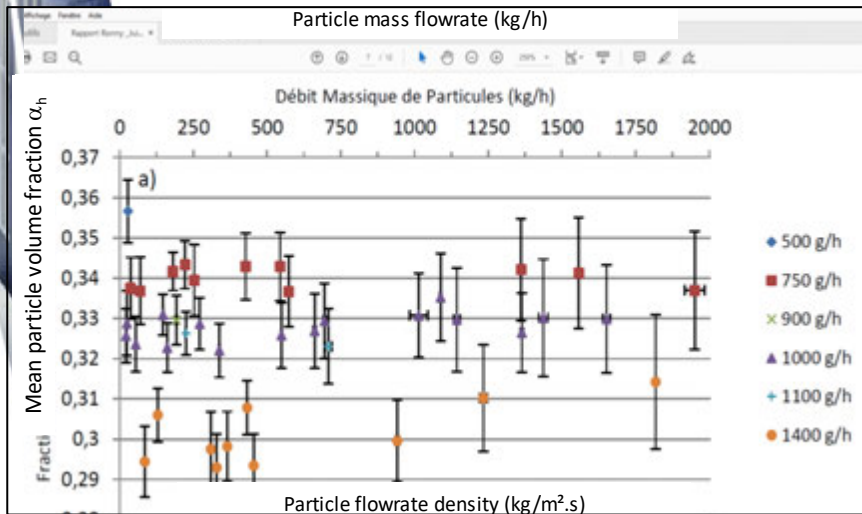
- Averaged particle volume fractions α_h are calculated from ΔP_{total}
- Local particle volume fractions α_i are calculated from ΔP_x



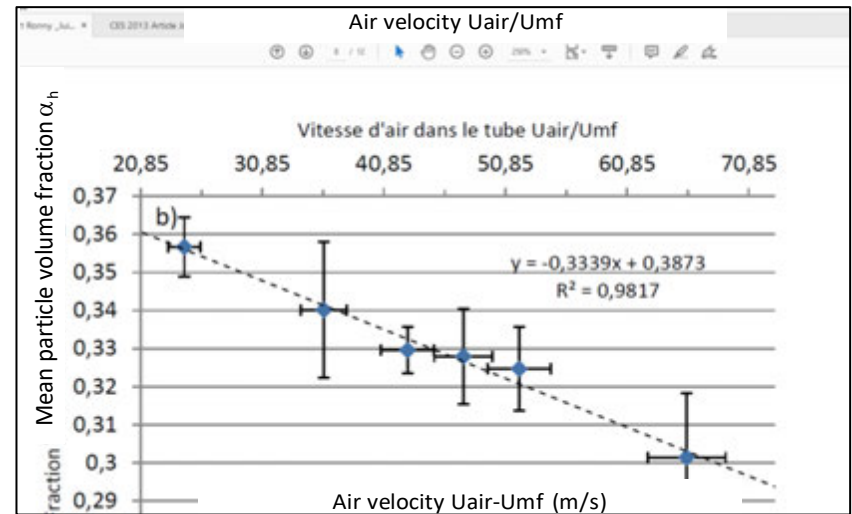
More than 40 experiments have been conducted to study the evolution of the particle volume fraction as a function of the particle mass flowrate and the air velocity.

Results :

- The system enables to manage high particle mass flowrate. No limitations were observed up to 350 kg/m².s (0.55 g/s) per 46mm ID tube.
- The particle volume fraction is ranged from 29% to 36%
- The mean particle volume fraction α_h is not dependent on the particle flowrate.
- Nevertheless, the aeration airflow rate affects the suspension density, the higher the airflow the lower the density.

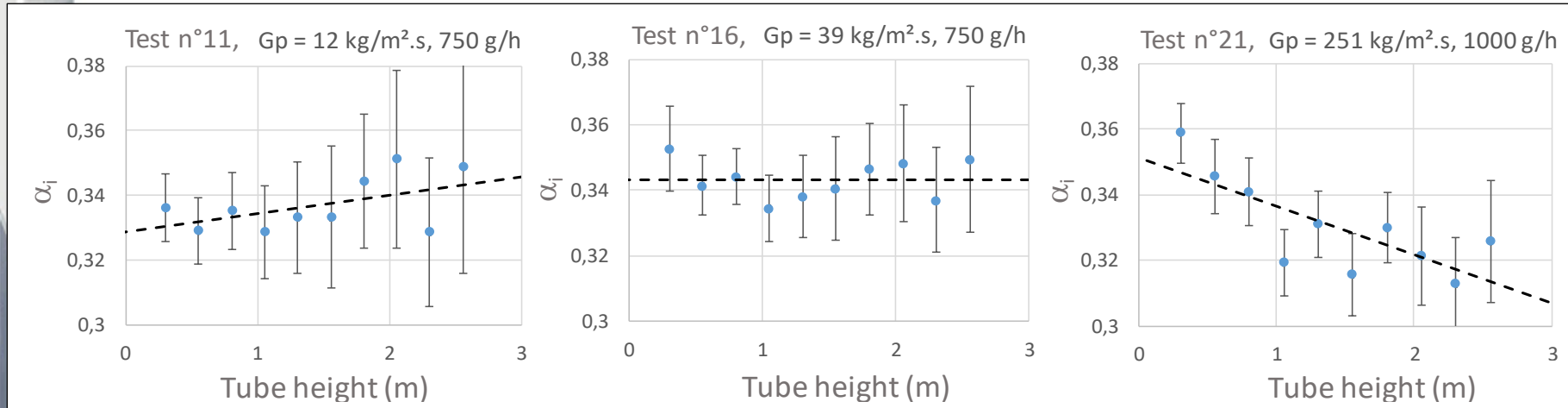


Averaged particle volume fraction over the tube height (α_h) as a function of the particle flowrate for several aeration air flowrate.



Averaged particle volume fraction over the tube height as a function of the air velocity

Results :



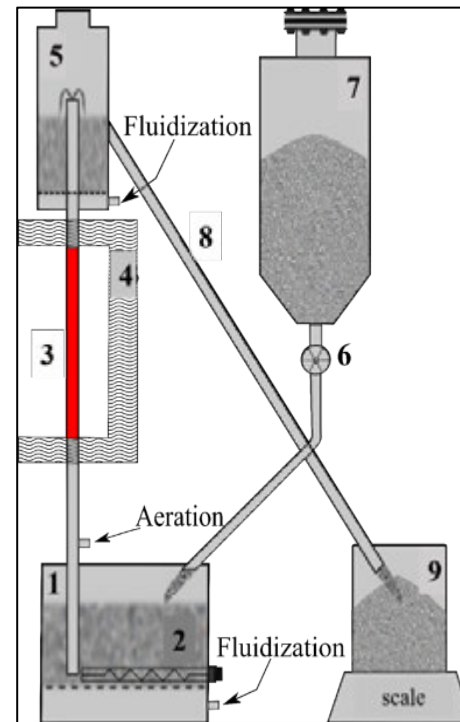
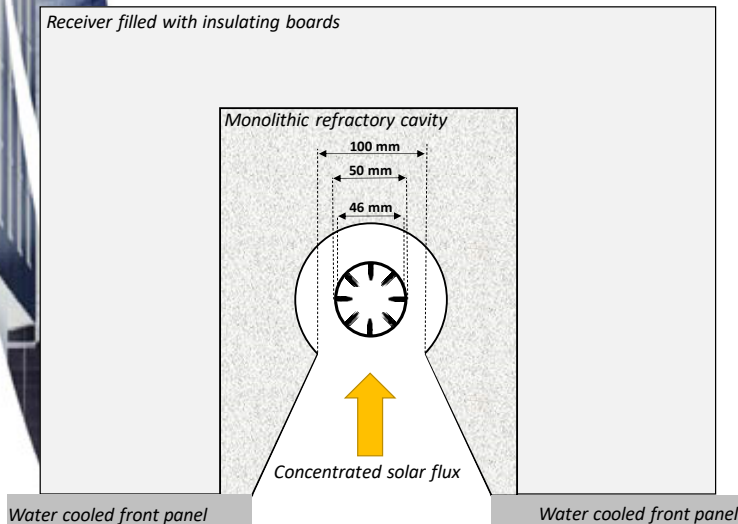
Examples of particle volume fraction evolution as a function of the tube height for several particle flowrate and air flowrate.

- The aeration does not influence the particle volume fraction distribution along the tube.
- The particle flowrate has a direct influence on this distribution.

↳ Particle volume fraction became lower at the top of the tube than at the bottom for particle mass flowrate higher than $40 \text{ kg/m}^2.\text{s}$

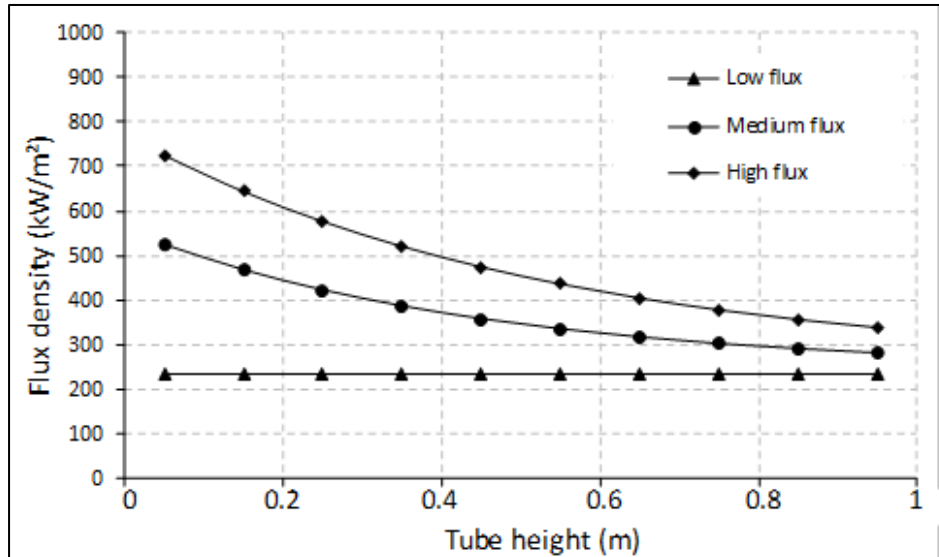
« On-sun » experimental setup :

- 1 m-long absorber finned tube coated with absorbing black paint (*Pyromark*[®])
- High refractory cavity
- Fluidized bed dispenser with a pressure control valve
- Secondary aeration at the bottom of the tube

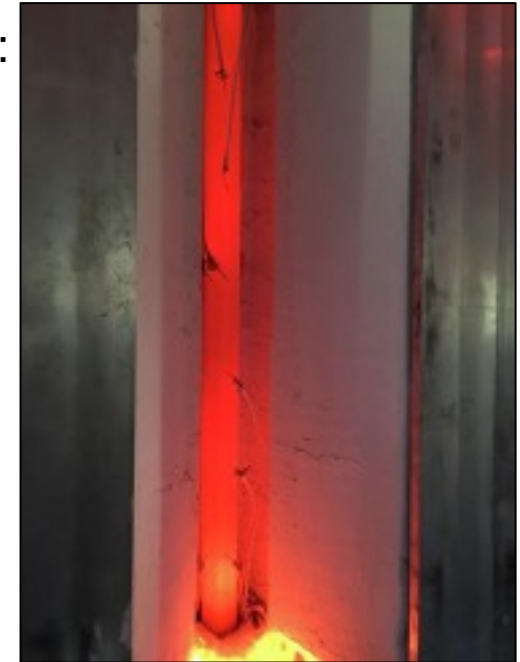


« On-sun » experimental setup :

- 3 solar flux distribution configurations were tested :

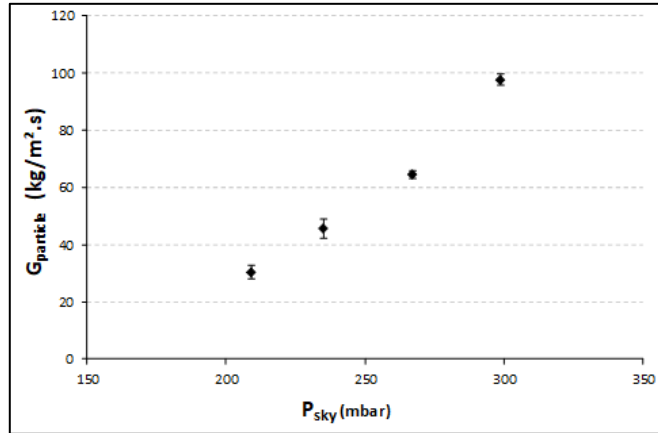


Solar flux densities distribution on the tube surface for the three different tested configurations (scaled to the reference DNI=1000 W/m²)



These three configurations (low, medium, high flux) correspond to mean solar flux densities of 236, 368 and 485 kW/m² respectively scaled to a 1000 W/m² DNI.

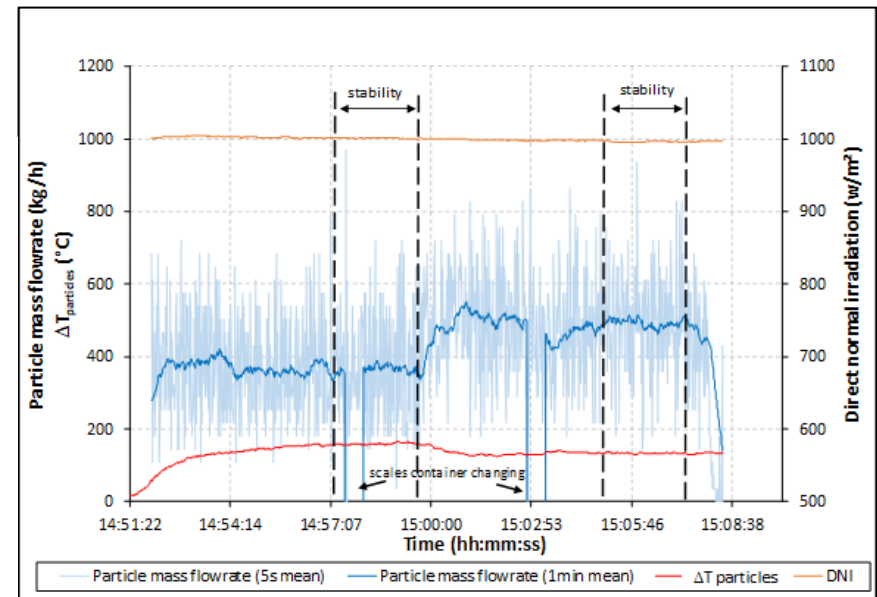
« On-sun » experimental setup :



Particle mass flow rate as a function of the dispenser freeboard pressure for the low solar flux configuration

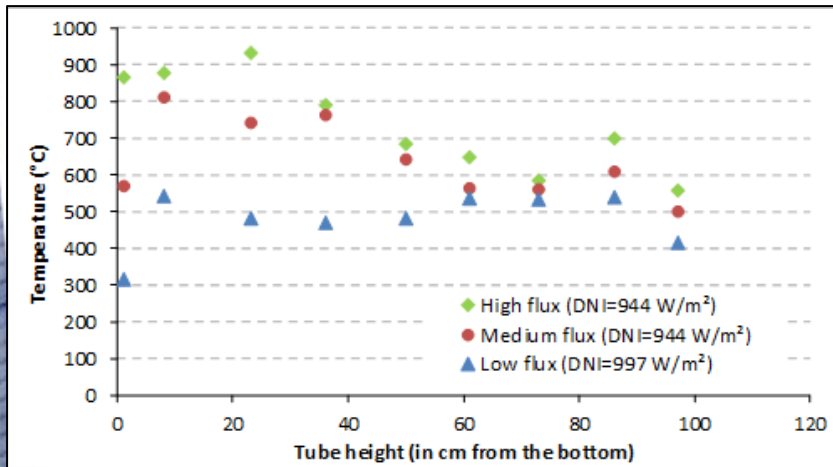
The particle flowrate is control through the dispenser freeboard pressure.

- The duration of each experiment depends on the time needed to reach the thermal steady state.
- The direct normal irradiation must be stable as well as the particles mass flow rate, and wall and particle temperatures.
- We defined a stability duration of two minutes to consider data as reliable.



Example of experimental data obtained during the on-sun campaign

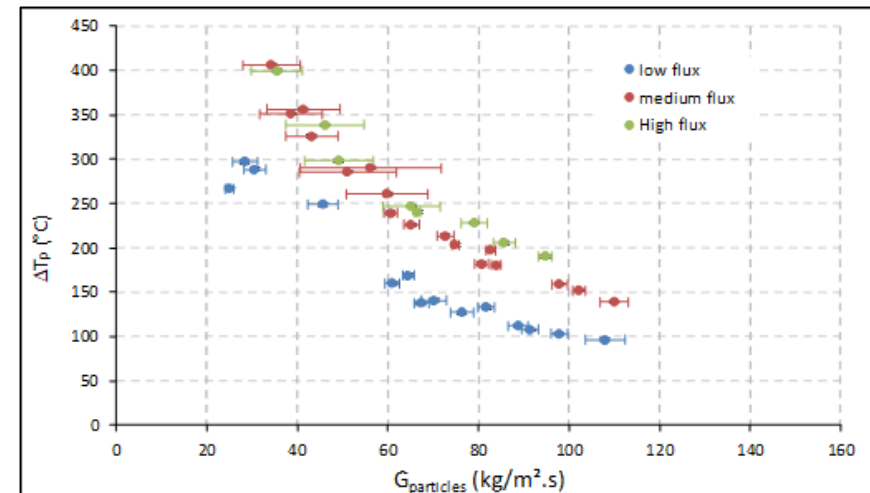
Temperature measurements :



Front wall temperature profile as a function of direct solar flux density; particle mass flow rate of $83 (\pm 2) \text{ kg/m}^2 \cdot \text{s}$.

- Particles temperature increase are measured between the dispenser and the end of the irradiated part of the tube
- The higher the particles mass flow rate, the lower the particle temperature increase
- Temperature increase of 400°C are reached with the 1m-long tube for high solar flux and small particles flowrate.

- Front wall temperature are measured along the tube height for the 3 solar flux density
- Temperature up to 930°C are reached with the high solar flux and a particle mass flowrate of $83 \text{ kg/m}^2 \cdot \text{s}$



Particle temperature increase between the inlet and the outlet of the irradiated cavity as a function of particle mass flow rate for different solar fluxes.

Power absorbed by particles :

$$\Phi_{DPS} = F_p \cdot C_{p,p} \cdot (T_{p,o,center} - T_{p,i,DiFB})$$

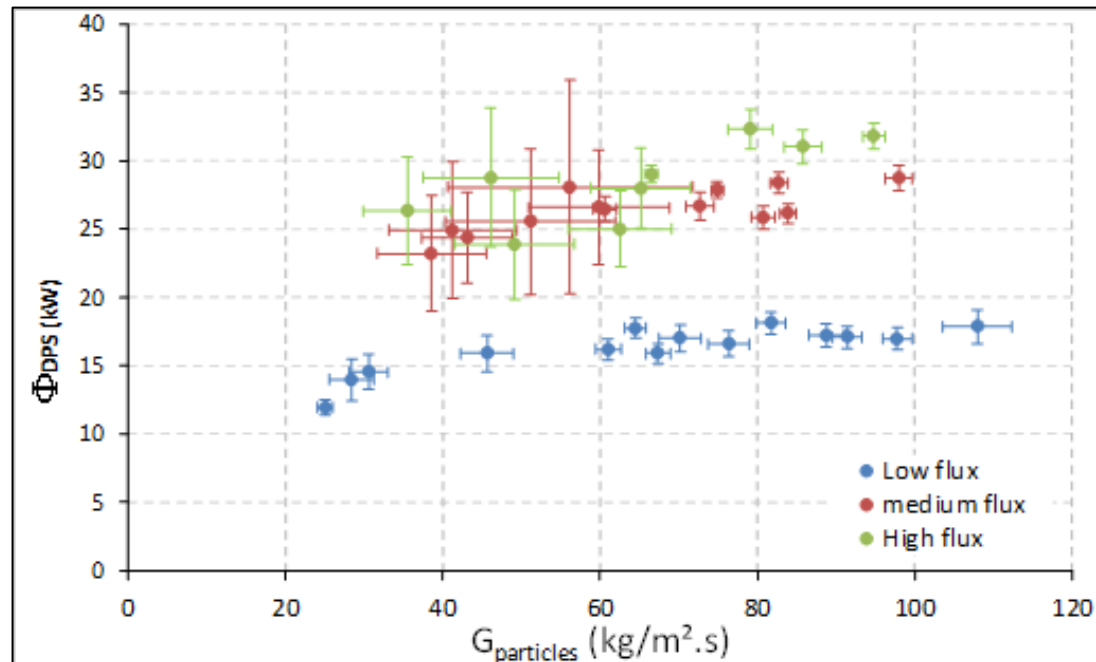
With:

F_p : the particles mass flow rate in kg/s

$C_{p,p}$: the heat capacity of olivine at the mean temperature

$T_{p,o,center}$: the particle temperature at the tube outlet

$T_{p,i,DiFB}$: the particle temperature in the dispenser fluidized bed



Power extracted by particles as a function of the particle mass flow rate and solar power input. Φ_{DPS} are scaled at a DNI of 1000 W/m².

Global heat transfer coefficient :

$$h_{tube} = \Phi_{DPS} / (A \cdot \Delta T_{lm})$$

With,

Φ_{DPS} : from eq.4

A: the internal surface area of the irradiated part of the receiver tube

ΔT_{lm} : the logarithmic mean temperature difference

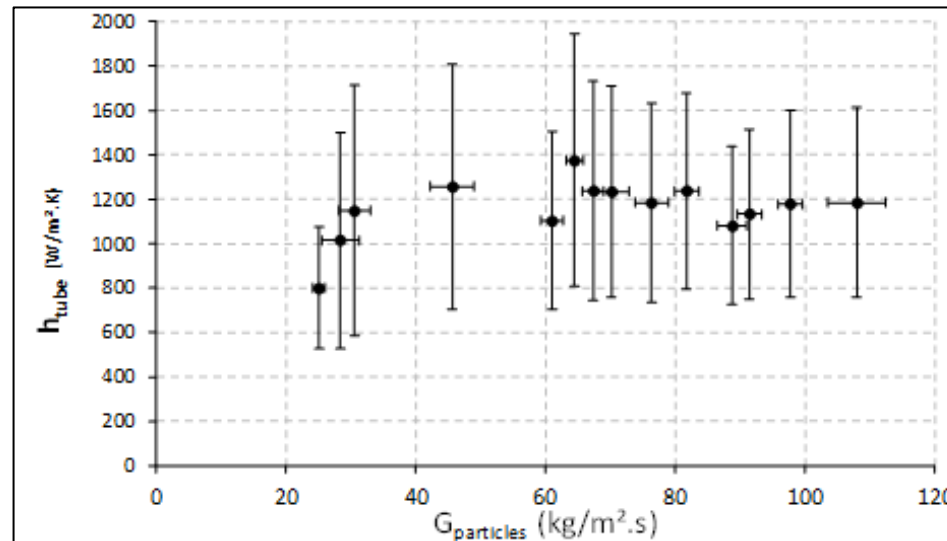
$$\Delta T_{lm} = \frac{(T_{w,i}^{int} - T_{p,i}) - (T_{w,o}^{int} - T_{p,o})}{\ln \frac{T_{w,i}^{int} - T_{p,i}}{T_{w,o}^{int} - T_{p,o}}}$$

With,

$T_{w,i/o}^{int}$: the internal wall temperature (inlet/outlet)

$T_{p,i}$: the inlet particles temperature

$T_{p,o}$: the outlet particles temperature



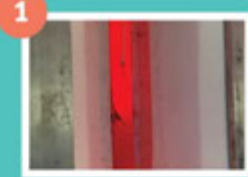
Heat transfer coefficient between the fluidized particles and the finned tube calculated as a function of the particles mass flux density at low solar flux.

- The system enables to manage high particle mass flowrate. No limitations were observed up to $350 \text{ kg/m}^2\cdot\text{s}$ (0.55 kg/s per 46mm ID tube).
- A secondary aeration is useful to stabilize the bubbling fluidization regime in tube. (to avoid slugging)
- The particle volume fraction is ranged from 29% to 36% and is not dependent of the particle mass flowrate.
- Dense suspension = Low particle velocity
↳ No attrition problems
- The global heat exchange coefficient, h_{tube} is $1200 \text{ W/m}^2\cdot\text{K}$
- The aeration does not show any influence on heat exchange because two effects counter balance. The higher the airflow, the higher the particle mixing which favors heat exchange but the higher the airflow, the lower the particle volume fraction that reduces heat exchange

High Temperature concentrated solar thermal power plant with particle receiver and direct thermal storage

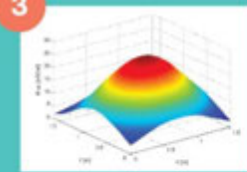
Heat transfer in solar-heated 1m-long receiver tube

Bare tube and fine tube testing. Temperature distribution and heat transfer coefficient.
June 2017 - January 2019



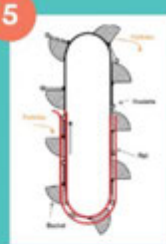
Solid flow regime in long tubes

Measurement of the transition between bubbling and slugging regimes.
December 2017



Concept for a 150 MW solar power plant based on the particle technology

Conceptual design of a multi-tower 150 MW solar power plant with particle circulation.
November 2018



Construction of the solar loop components

Manufacturing of the solar receiver, the heat exchanger and the storage bins.
January 2019



Complete solar loop testing

Testing and performance evaluation of the particle solar loop.
February 2020

Starting the pilot loop testing

Definition of the parameters for circulating the particles in close loop.
September 2019

PROJECT STARTING
OCTOBER 2016

2017

2018

2019

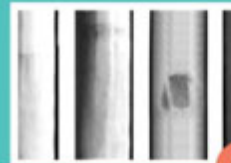
TO BE COMING SOON

PROJECT ENDING
SEPTEMBER 2020



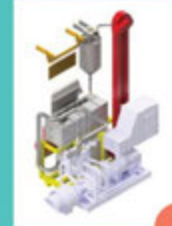
High efficiency thermodynamic cycles

Selection of various cycles that can reach 50% efficiency.
November 2017



Design of the pilot loop to be tested

Design of all the components of the loop to be tested atop the Themis solar tower and integration in the focal zone.
March 2018



Themis solar field performance assessment

Design, construction and implementation of a moving bar for measuring the solar flux distribution at the solar receiver aperture.
December 2018



Delivery of the solar loop components at Themis site

Delivery and lifting of the main solar loop components.
May 2019

9

Testing of the solar receiver

Measurement of the solar receiver efficiency.
November 2019

10

11

12

Full system testing

Testing and performance evaluation of the complete loop including the turbine.
June 2020



- This project has received funding from the European Union's Horizon H2020 research and innovation programme under grant agreement No 727762, Next-CSP project
- The French "Investments for the future" program managed by the National Agency for Research under contracts ANR-10-EQPX-49 (SOCRATE) supported the facility.
- The Occitanie French region funded the cold mockup.

